Review article Available online www.ijsrr.org ISSN: 2279–0543

International Journal of Scientific Research and Reviews

Graphite/Mno_2 Nanocomposites Assisted with PVA and PVP as Cathodic Active Materials

Shanmugam V[1], Vinitha M[1], Revathi S[1], Vishnudevan M[2], Seethalakshmi T[1*]

[1]Department of Physics, Government Arts College, Karur 639005, Tamil Nadu, India.
[2]Department of Chemistry, Government Arts College, Karur 639005, Tamil Nadu, India

ABSTRACT

MnO_2 nanoparticles were synthesized using $MnCl_2$ precursors with $KMnO_4$ by hydrothermal method. The same method was repeated for the synthesis of Graphite/MnO_2, Graphite/MnO_2/PVA and Graphite/MnO_2/PVP Nano composites. XRD, FE-SEM ,UV Visible, Raman and FTIR spectroscopic studies were carried out to characterize as synthesised MnO_2 nanoparticles and Nano composites. From XRD pattern it was confirmed that the presence of alpha-MnO_2 nanoparticles and UV -Visible studies revealed that the band gap energy drastically reduced when PVA and PVP added in to the Graphite/ MnO_2 nanoparticles, this was due to the conductance performance of the PVA and PVP polymers. Cyclic Volta metric study confirmed the shifting of potential to more cathodic for PVA and PVP assisted Graphite/ MnO_2 nanoparticles. The MnO_2 nanoparticles usually used as a anodic active materials for many primary batteries but we find in our CV study the Graphite / MnO_2/PVA and Graphite/ MnO_2/PVP Nano composite materials can be used as cathodic active materials.

KEY WORDS:MnO_2NPs,Graphite/MnO_2/PVP Nano composites, FE-SEM, CV study.

*Corresponding Author

Dr.T.Seethalakshmi,

Department of Physics,

Government Arts College, Karur 639005, Tamil Nadu, India

Email: **nvsgacphy@gmail.com**

1. INTRODUCTION

In recent years power and energy industries demands more efficient and effective portable electronic devices such as roll-up displays, photovoltaic cells, and wearable devices[1–4] etc. Currently, cathode electrodes materials were more attracted than the development anodic electrode materials[5.] Manganese oxides are used most widely as electrode material for design of batteries [6], electrochemical pseudocapacitors[7,8] and electrochemical cells[9]. Among the attractive anode materials, manganese dioxide has emerged as an effective alternative to graphite anodes because it offers an extremely high theoretical specific capacity of 1230 $mAh \cdot g^{-1}$ and excellent electrochemical behavior, alongside its low price, natural abundance and environmental friendliness[10,11,12] but it suffers from significant capacity loss and poor cyclic stability due to the large volume expansion during cycling, which limit its widespread application[13,14]. To meet out such challenges, tremendous work has been focused on the most popular method of building nanostructured materials based on Manganese oxide nanomaterial's .

The capacitances of manganese oxide electrodes are limited because of its poor electrical conductivity[15]. To enhance the electrical conductivity and charge-storage capability of manganese oxide electrodes, modifications have to be carried out—for instance, adding to the electrode other transition metal elements such as Ni, Cu and Fe or metallic elements such as Al or Sn[16,17,18]. Another method of electrode modification is the deposition of manganese oxides on porous and high-surface-area materials with an electronically conducting structure. Carbon nanofoams, Nano graphite and template mesoporous carbon are especially used for this process[19]. Manganese oxides are used most widely as electro design batteries[20], electrochemical pseudo capacitors [21,22] and electrochemical cells[23]. Among the attractive anode materials, manganese dioxide has emerged as an effective alternative to graphite anodes because it offers an extremely high theoretical specific capacity of 1230 $mAh \cdot g^{-1}$ and excellent electrochemical behavior, alongside its low price, natural abundance and environmental friendliness [24,25,26], but it suffers from significant capacity loss and poor cyclic stability due to the large volume expansion during cycling, which limit its widespread application[27,28]. To meet such challenges, tremendous work has been focused on the most popular method of building nanostructured materials.

The capacitance of manganese oxide electrodes is limited because of its poor electrical conductivity [29]. To enhance the electrical conductivity and charge-storage capability of manganese oxide electrodes, modifications have to be carried out—for instance, adding to the electrode other transition metal elements such as Ni, Cu and Fe or metallic elements such as Al or Sn [30,31,32]. Another method of electrode modification is the deposition of manganese oxides on porous and high-surface-

area materials with an electronically conducting structure. Carbon nanofoams, Nano graphite and template mesoporous carbon are especially used for this process [33].

In this work, steps have been taken to enhance the conductivity of the MnO_2 nanoparticles which are assisted on natural graphite through the hydrothermal method. In addition to that Graphite/MnO_2 nanoparticles are embedded with polyvinyl alcohol and polyvinyl pyrrolodine polymers separately. Recently in one study, for the fabrication of super capacitor a cathodic layer of graphite was made[34]. Based on the above considerations, in this study, we develop a Graphite/MnO_2, graphite/MnO_2/PVA and Graphite/MnO_2 /PVP Nano composites by hydrothermal method. Accordingly the natural graphite PVA and PVP layers can obviously enhance the conductivity of MnO_2 nanoparticles and it will provide electron "super highways" for charge storage and delivery because of its excellent electrical conductivity, which will overcome the key weakness (the limited electric conductivity) of MnO_2 and further enhance the conductivity of electrode MnO_2 nanoparticles has been recognized as the most promising electrode material for SCs[35–39]. The MnO_2 can provide a greatly enhance the electro active surface area. Recent work shows that SCs based on MnO_2 films grown on conductive substrates exhibit high performance[40–43]. Electrochemical measurements show that the designed graphite/MnO_2/PVA and graphite/MnO_2/PVP Nano composites exhibit high performance. Manganese oxides are characterized as nontoxic and efficient catalytic materials that are easy to synthesize [44].

2. MATERIALS AND METHODS

2.1 Materials used

All the chemicals used in the experiments were of analytical grade without further purification. Natural graphite fine powder (98%) was purchased from Lobe Chem. $KMnO_4$(≥99%) from Sigma Aldrich. $MnCl_2$, PVA, PVP (K-30) and ethanol solutions were purchased from Merck Ltd.

2.2. Synthesis of Graphite oxide

A mixture of 0.34 gram of $MnCl_2$ and 0.2gram of $KMnO_4$ were dissolved into the 50 ml of ethanol. These solution were subjected to reflux process under 78^0C for a period of 8 hrs. During the process after half an hour a small amount of natural graphite flake was added to the solution. Similarly the same procedure was repeated while the preparation of graphite/MnO_2/PVA and PVP and it was left in the stirrer for several hours. Then the obtained filtrate is then washed with HCl. Then the dark yellow colour suspension was obtained. The obtained solution was dried under vacuum at 50^0 C for 24 hours. Thus, the dried mixture of graphite rods were collected finally.

3. RESULTS AND DISSCUSSION

3.1. X-ray Diffraction (XRD)

The X-ray diffraction of the synthesized Graphite/MnO_2 Nano composite , Graphite/MnO_2 with PVA, PVP Nano composite were recorded on XPERT-PRO diffract meter system equipped with a Cu (kα) radiation source(λ=1.5406Å) as shown in the figure(3.1).

Average crystallite size was calculated using Debye-Scherer formula,

$$D = \frac{k\lambda}{\beta cos\theta} \quad (m)$$

Where,

D - Average crystallite domain size (m),

λ- Wavelength of X – rays (1.54060×10^{-10} m)

β -Full width half maximum (radian)

θ - Diffraction angle (degree)

K -0.94

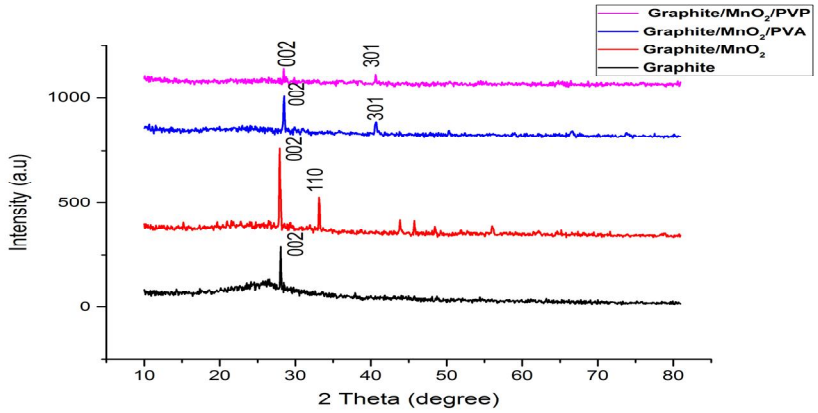

Fig-1. X-ray diffraction pattern of Graphite, Graphite/MnO_2, Graphite/MnO2/PVA and Graphite/MnO_2/PVP

The phase purity and the crystalline structure of the as-prepared graphite/MnO_2, graphite/MnO_2/PVA and graphite/MnO_2/PVP nanoparticles were examined by the XRD pattern as shown in fig(3.1). Hence the presence of graphite was observed to be (002) planes of graphite in the range of 22-28^0 for every prepared samples of Graphite, Graphite/MnO_2 Graphite/MnO_2/PVA, Graphite/MnO_2/PVP[45],the small peaks of MnO_2 was observed at 40.54,corresponds to(301) plane. This plane strongly attributes the presence of MnO_2 nanoparticles in Graphite nanocomposites[46,47]. The Average crystal size of the synthesized Graphite, Graphite/MnO_2, Graphite/MnO_2/PVA and Graphite/MnO_2/PVP were of 20nm, 231nm, 525nm and 651nm respectively [48].

3.2 UV-Visible absorption spectral analysis

The UV-Visible absorption of synthesized samples were recorded by perking-Elmer lambda 35 spectrometer with a variable radiation wavelength between 200 to 1200nm as shown in the Fig (3.2). It depicts the optical spectra of the synthesized Graphite, Graphite/MnO_2, Graphite/MnO_2/PVA and Graphite/MnO_2/PVP Nano composite. The absorption peak at UV region was used to study the shifting in optical band gap energy for the synthesized materials.

The optical energy band gap E_g was calculated from the Tauc's relation

$$\alpha h\nu = A\,(h\nu - Eg)^n$$

where,

A-constant

α-Absorbtion co efficient of the material

Eg-band gap energy (eV)

n-the power factor and that take 1/2, 2, 3/2 and 3 allowed direct, allowed indirect forbidden direct and forbidden indirect transitions respectively.

The optical band gap were found to be 2.33, 1.90, 1.80,and 1.77 eV for Graphite, Graphite/MnO_2, Graphite/MnO_2/PVA and Graphite/MnO_2/PVP respectively[49,50] The optical band gap decreases as shown in fig-2.

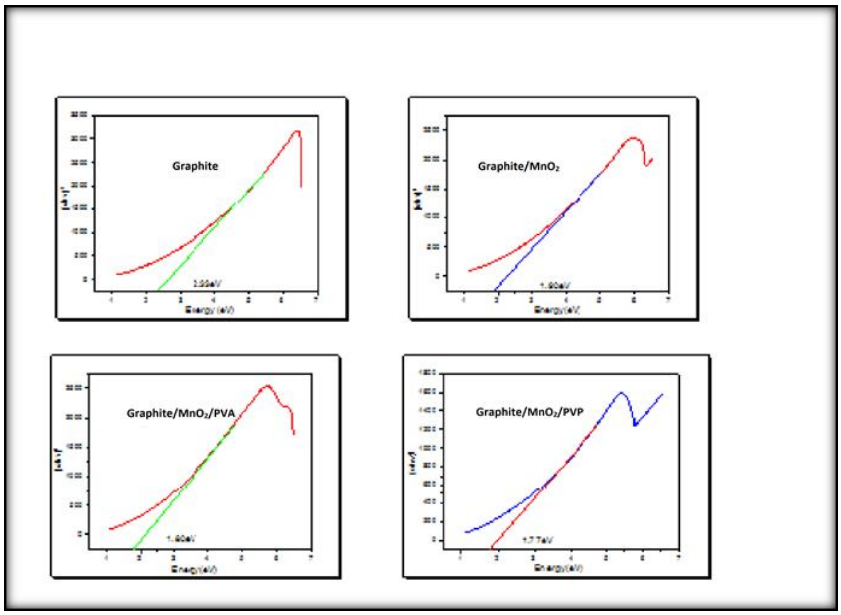

Fig-2. UV-Vis spectra for Graphite, Graphite/ MnO_2, Graphite/MnO_2/PVA and Graphite/MnO_2/PVP nanocomposite.

3.3. Raman spectroscopy analysis

Raman spectroscopy is a non destructive technique. Raman spectrum helps to determine the vibration of phonons in the lattice structures. The frequency of vibrations of the material depends on the atomic masses and its bond strength. This Raman Effect is due to the interaction of electromagnetic field of the incident beam with the given sample material. If the laser light falls on the sample it may interact in different forms such as absorption, scattering or reflection [51.] Heavy atoms and weak bonds contain low raman vibrations, light atoms and strong bonds contains high raman vibrations.

The inelastic scattering of photon known as Raman Effect. Thus the higher energy wavelength referred as Anti stokes lines and lower wavelength referred as stokes scattering [52.] Due to instability returns to its initial state and it emits photons of same energy, it is termed to be Rayleigh's scattering. The size of sp^2 ring clusters in a sp^3 hybrid network of carbon atom can be determined by the intensity of ratio of the D and G band (ID/IG)[53.]The D-band is related to degree of disorder in graphite and while G-band is related to C-C vibrational mode.

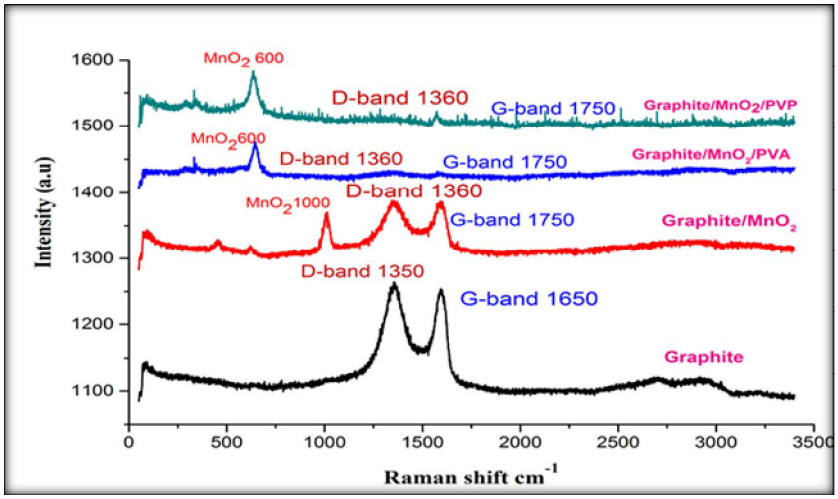

Fig-3. Raman spectra for Graphite, Graphite/MnO_2, Graphite/MnO_2/PVA Graphite/MnO_2/PVP Nano composite.

The Raman spectra of all Graphite Nano composites contain both D and G bands. The above graph displays the raman spectra of Graphite reveals that presence of very strong D peak at (1350-1360)cm^{-1} which shows that disorder of the sample and also displays the G-band around (1650-1750)cm^{-1},the peak around (650-1000)cm^1 Shows the presence of MnO_2 nanoparticles. The intensity values of I(D)/I(G) of synthesized Graphite, Graphite/MnO_2, Graphite/MnO_2/PVA and Graphite/MnO_2/PVP are 0.18, 0.25, 0.25, 0.25. I(D)/I(G), rationalize reciprocally with the size of crystalline grains [54]. If the number of layers is smaller than five then the peak becomes more intense

than G peak. Therefore the Raman effect is due to interaction of electromagnetic field of incident beam with sample materials.

3.4. Fourier Transform infra-red spectroscopy (FTIR)

The FT-IR spectrum of Graphite, Graphite/ MnO2, Graphite/MnO2/PVA and Graphite/MnO_2/PVP was shown in fig-4.

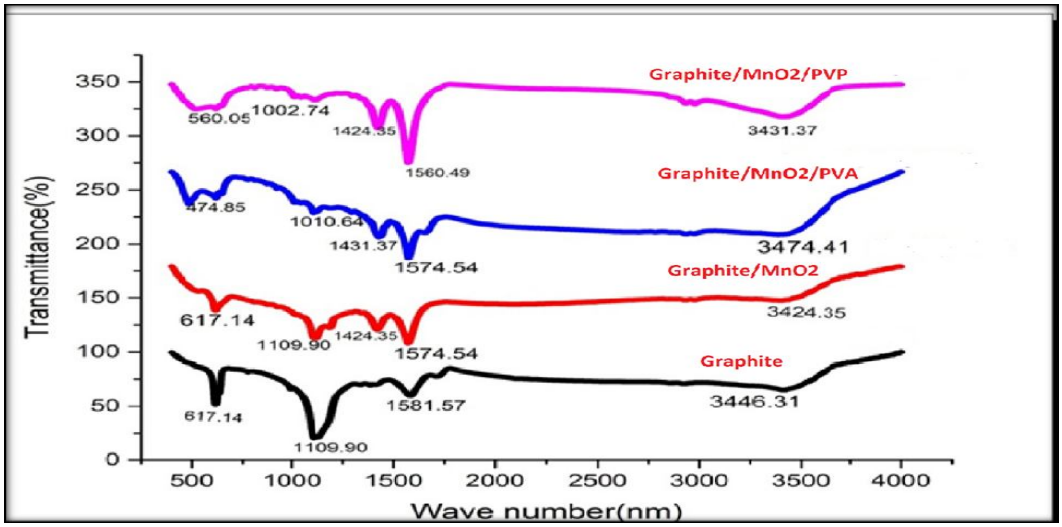

Fig-4. FT-IR spectrum of Graphite, Graphite/ MnO2, Graphite/MnO2/PVA and Graphite/MnO_2/PVP nanocomposite

From the above fig-4, the typical broad absorption in the wave length ranges above 3400 cm^{-1} are allocated for O-H stretching, Which denotes the peaks corresponding to the wave number above 1570cm^{-1} denoting the presence of functional groups such as O-C-O,C=C respectively. The number of oxygen containing functional groups is comparatively low in graphite. As such, it can be implicated that the Graphite contains very less amount of O-H groups, which are yet corresponding to structural OH groups or physically absorbed water from the atmosphere during the analysis or completely reduced carboxylic groups to alcohols. However, the water absorption did not takes place significantly due to the non-polar nature of graphite, The appearance of a new peak in the region of 1560-1581 cm^{-1} attributes to the skeletal vibrations from un-oxidized graphitic domains (aromatic regions of GO) or graphite [55].

3.5. Scanning Electron Microscope (SEM)

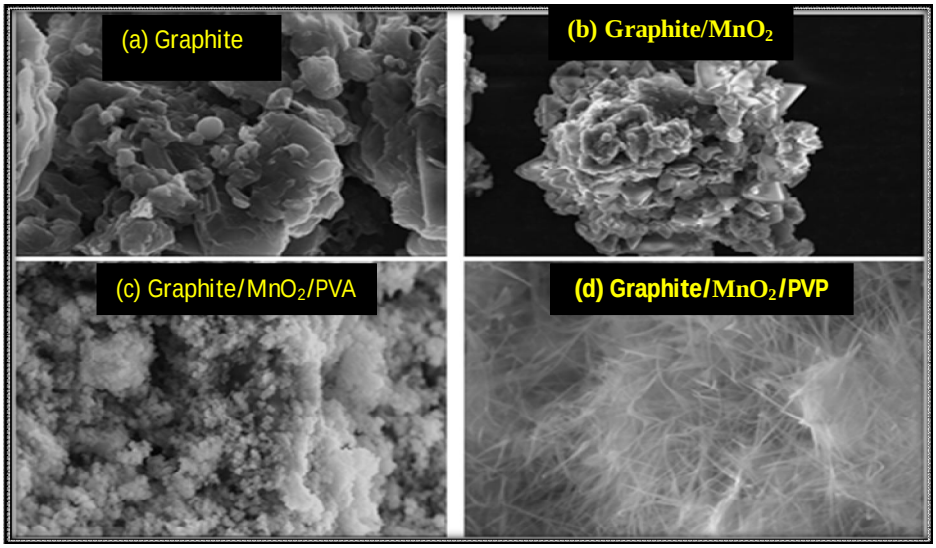

Fig-5. FE-SEM of Graphite, Graphite/ MnO2, Graphite/MnO2/PVA and Graphite/MnO_2/PVP.

Fig-[5a&b] shows that FESEM images of the Graphite, Graphite/MnO_2, which reveals that MnO_2 nanoparticles were decorated and dispersed on the Graphite sheets. The morphology of the synthesized materials were entirely changed. Graphite/MnO_2/PVA and Graphite/MnO_2/PVP nanocomposite appears like MnO_2 nano-needle structure on the graphite sheets. In addition to that, it can be observed that most of the Graphite/MnO_2 Nano composites have a triangular shape, that MnO_2 triangular nanoparticles were decorated as the petals of rose flower of graphite sheets.

3.6. Cyclic voltammetry

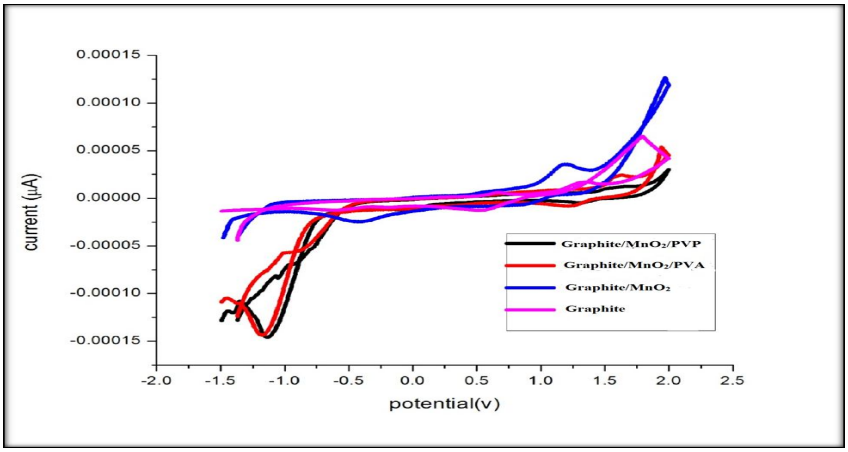

Fig-6. Cyclic Voltammeter of Graphite, Graphite/ MnO_2, Graphite/ MnO_2/PVA and Graphite/MnO_2/PVP Nano composite.

The Cyclic Voltammeter was recorded by Princeton applied research (2 channels) frequency ranges from 1Hz to 1MHz. The Cyclic voltammetry is the most widely used technique for acquiring qualitative information about electrochemical reactions. The power of cyclic voltammetry results from its ability to provide considerable information on redox processes and the kinetics of heterogeneous electron-transfer reactions, and on coupled chemical reactions or adsorption processes. Cyclic voltammetry is often the first experiment performed in an electro analytical study. In particular, it offers a rapid location of redox potentials of the electro active species. The anodic and cathodic peak of cv are arranged parallel to each other. Here, positive current shows the oxidation and negative current shows the reduction behaviors. Hence different areas and reduction behavior of graphite samples depends upon shape, size and thickness of film, which leads to reduction current of the electrode materials. The peaks of cv broadens as compared to graphite and graphite/MnO_2. Thus the shape of cv curve gives the reversible charge-discharge behavior [56]. It is evident that all CV scans recorded from -1.5 to 2.5V. The cathodic potential of synthesized Graphite, Graphite/MnO_2, Graphite/MnO_2/PVA and Graphite/MnO_2/PVP were analyzed 1V, 0.2V, -0.8V,-0.9V respectively, which indicates cathodic potential were dramatically tuning from +1V to -0.9V. This changes were obtained from nature of the polymers.

CONCLUSION

Graphite/MnO_2 Nano composite without and with assisted by PVA and PVP nan composites were successfully synthesized by hydrothermal method. The XRD patterns revealed that graphite/MnO_2 present in our synthesized Nano composites. Raman spectrum confirmed the presence of graphite/MnO_2 nanoparticles, when graphite/MnO_2 embedded on PVA and PVP the interfacial peak intensity was decreased. The optical band gap energy and catholic potential of graphite/MnO_2 were tuned for PVA, PVP assisted Nano composite which leads to enhance electronic properties of the nan composite.

REFERENCES

1. Y. Qin, X. D. Wang and Z. L. Wang, Nature, 2008; 451: 809–813.
2. K. Wang, Q. Meng, Y. Zhang, Z. Wei and M. Miao, Adv. Mater., 2013; 25:1494–1498.
3. Y. L. Yuan, B. Yao, B. Hu, K. F. Huo, W. Chen and J. Zhou, Energy Environ. Sci., 2013; 6:470–476.
4. Y. Li, Z. Li and P. K. Shen, Adv. Mater., 2013; 25: 2474–2480.2480.
5. L. Yuan, X. Xiao, T. Ding, J. Zhong, X. Zhang, Y. Shen, B. Hu, Y. Huang, J. Zhou and Z. L. Wang, Angew. Chem., Int. Ed.,2012; 51: 4934–4938.

6. Zhang K., Han X., Hu Z., Zhang X., Tao Z., Chen J. Nanostructured Mn- based oxides for electrochemical energy storage and conversion. Chem. Soc. Rev. 2015;44:699–728. doi: 10.1039/C4CS00218K. [PubMed] [Cross Ref].
7. Huang M., Li F., Dong F., Zhang Y.X., Zhang L.L. MnO_2-based nanostructures for high-performance super capacitors. J. Mater. Chem. A. 2015;3:21380–21423.doi: 10.1039/C5TA05523G. [Cross Ref]
8. Cao J., Li X., Wang Y., Walsh F.C., Ouyang J.-H., Jia D., Zhou Y. Materials and fabrication of electrode scaffolds for deposition of MnO_2 and their true performance in super capacitors. J. Power Sources. 2015;293:657–674. doi: 10.1016/j.jpowsour.2015.05.115. [Cross Ref]
9. Bélanger D., Brousse T., Long J.W. Manganese oxides: Battery materials make the leap to electrochemical capacitors. Electrochemist. Soc. Interface. 2008;17:4952.
10. Cai M., Qian H., Wei Z., Chen J., Zheng M., Dong Q. Polyvinyl pyrrolidone-assisted synthesis of a Fe_3O_4/graphene composite with excellent lithium storage properties. RSC Adv. 2014;4:6379–6382. doi: 10.1039/c3ra45993d. [Cross Ref]
11. Dong Y.C., Ma R.G., Hu M.J., Cheng H., Tsang C.K., Yang Q.D., Li Y.Y., Zapien J.A. Scalable synthesis of Fe_3O_4 nanoparticles anchored on grapheme as a high-performance anode for lithium ion batteries. J. Solid State Chem. 2013;201:330–337.doi: 10.1016/j.jssc.2012.12.021. [CrossRef]
12. Zhang X., Wang T., Jiang C., Zhang F., Li W., Tang Y. Manganese dioxide/carbon nanotubes composite with optimized microstructure via room temperature solution approach for high performance lithium-ion battery anodes. Electro him. Acta. 2016;187:465–472. doi: 10.1016/j.electacta.2015;11:084. [Cross Ref]
13. Dong Y.C., Ma R.G., Hu M.J., Cheng H., Tsang C.K., Yang Q.D., Li Y.Y., Zapien J.A. Scalable synthesis of Fe_3O_4 nanoparticles anchored on grapheme as a high-performance anode for lithium ion batteries. J. Solid State Chem. 2013;201:330–337.doi: 10.1016/j.jssc.2012.12.021. [Cross Ref]
14. Li J., Zhao Y., Wang N., Ding Y., Guan L. Enhanced performance of a MnO_2-graphene sheet cathode for lithium ion batteries using sodium alginate as a binder. J. Mater. Chem. 2012;22:13002–13004. doi: 10.1039/c2jm31583a. [Cross Ref]
15. Wei W., Cui X., Chena W., Ivey D.G. Manganese oxide-based materials as electrochemical super capacitor electrodes. Chem. Soc. Rev. 2011;40:1697-1721.doi:10.1039/C0CS00127A. [PubMed] [Cross Ref]

16. Chen Y.S., Hu C.C. Capacitive characteristics of binary manganese-nickel oxides prepared by anodic deposition. Electrochemist. Solid State Lett. 2003;6:A210–A213. doi: 10.1149/1.1601373. [Cross Ref]
17. Kim H., Popov B.N. Synthesis and characterization of MnO_2-based mixed oxides as super capacitors. J. Electrochem. Soc. 2003;150:D56–D62.doi: 10.1149/1.1541675. [Cross Ref]
18. Li Y., Xie H.Q. Mechano chemical-synthesized Al-doped manganese dioxides for electrochemical supercapacitors. Ionics. 2010;16:21–25.do10.1007/s11581-009-0325-5. [Cross Ref]
19. Fischer A.E., Pettigrew K.A., Rolison D.R., Stroud R.M., Long J.W. Incorporation of homogeneous, Nano scale MnO_2 within ultra porous carbon structures via self-limiting electro less deposition: Implications for electrochemical capacitors. Nano Lett. 2007;7:281–286. doi: 10.1021/nl062263i. [PubMed] [Cross Ref]
20. Zhang K., Han X., Hu Z., Zhang X., Tao Z., Chen J. Nanostructured Mn-based oxides for electrochemical energy storage and conversion. Chem. Soc. Rev. 2015;44:699–728. doi: 10.1039/ C4CS00218K. [PubMed] [Cross Ref]
21. Huang M., Li F., Dong F., Zhang Y.X., Zhang L.L. MnO_2-based nanostructures for high-performance super capacitors. J. Mater. Chem. A. 2015;3:21380–21423. doi: 10.1039/C5TA05523G. [Cross Ref]
22. Cao J., Li X., Wang Y., Walsh F.C., Ouyang J.-H., Jia D., Zhou Y. Materials and fabrication of electrode scaffolds for deposition of MnO_2 and their true performance in super capacitors. J.Power Sources. 2015;293:657–674.doi:10.1016/j.jpowsour.2015.05.115. [CrossRef]
23. Bélanger D., Brousse T., Long J.W. Manganese oxides: Battery materials make the leap to electrochemical capacitors. Electrochemist. Soc. Interface. 2008;17:4952.
24. Cai M., Qian H., Wei Z., Chen J., Zheng M., Dong Q. Polyvinyl pyrrolidone-assisted synthesis of a Fe_3O_4/graphene composite with excellent lithium storage properties. RSC Adv. 2014;4:6379–6382. doi:10.1039/c3ra45993d. [Cross Ref]
25. Dong Y.C., Ma R.G., Hu M.J., Cheng H., Tsang C.K., Yang Q.D., Li Y.Y., Zapien J.A. Scalable synthesis of Fe_3O_4 nanoparticles anchored on graphene as a high-performance anode for lithium ion batteries. J. Solid State Chem. 2013;201:330–337. doi: 10.1016/j.jssc.2012.12.021. [Cross Ref]
26. Zhang X., Wang T., Jiang C., Zhang F., Li W., Tang Y. Manganese dioxide/carbon nanotubes composite with optimized microstructure via room temperature solution approach

for high performance lithium-ion battery anodes. Electrochim. Acta. 2016;187:465–472. doi: 10.1016/j. electacta. 2015.11.084. [Cross Ref]

27. Dong Y.C., Ma R.G., Hu M.J., Cheng H., Tsang C.K., Yang Q.D., Li Y.Y., Zapien J.A. Scalable synthesis of Fe_3O_4 nanoparticles anchored on grapheme as a high-performance anode for lithium ion batteries. J. Solid State Chem. 2013;201:330–337. doi: 10.1016/j.jssc.2012.12.021. [CrossRef]
28. Li J., Zhao Y., Wang N., Ding Y., Guan L. Enhanced performance of a MnO_2-graphene sheet cathode for lithium ion batteries using sodium alginate as a binder. J. Mater. Chem. 2012;22:13002–13004. doi: 10.1039/c2jm31583a. [Cross Ref]
29. Wei W., Cui X., Chena W., Ivey D.G. Manganese oxide-based materials as electrochemical super capacitor electrodes. Chem. Soc. Rev. 2011;40:1697–1721. doi: 10.1039/C0CS00127A. [PubMed] [Cross Ref]
30. Chen Y.S., Hu C.C. Capacitive characteristics of binary manganese-nickel oxides prepared by anodic deposition. Electrochem. Solid State Lett. 2003;6:A210–A213. doi: 10.1149/1.1601373. [Cross Ref]
31. Kim H., Popov B.N. Synthesis and characterization of MnO_2-based mixed oxides as super capacitors. J. Electroc hem. Soc. 2003;150:D56–D62. doi: 10.1149/1.1541675. [Cross Ref]
32. Li Y., Xie H.Q. Mechanochemical-synthesized Al-doped manganese dioxides for electrochemical super capacitors. Ionics. 2010;16:21–25. doi: 10.1007/s11581-009-0325-5. [Cross Ref]
33. Fischer A.E., Pettigrew K.A., Rolison D.R., Stroud R.M., Long J.W. Incorporation of homogeneous, Nano scale MnO_2 within ultra porous
34. G. Zheng, L. Hu, H. Wu, X. Xie and Y. Cui, Energy Environ.Sci., 2011;4:3368–3373.
35. Z. Yu, B. Duong, D. Abbitt and J. Thomas, Adv. Mater., 2013;25: 3302–3306.
36. L. B. Hu, J. W. Choi, Y. Yang, S. Jeong, F. La Mantia, L. F. Cuiand and Y. Cui, Proc. Natl. Acad. Sci. U. S. A., 2009;106: 21490–21494.
37. X. Lu, T. Zhai, X. Zhang, Y. Shen, L. Yuan, B. Hu, L. Gong,J. Chen, Y. Gao, J. Zhou, Y. Tong and Z. L. Wang, Adv. Mater., 2012; 24: 938–944.
38. J. Liu, J. Jiang, C. Cheng, H. Li, J. Zhang, H. Gong and H. J. Fan, Adv. Mater., 2011; 23: 2076–2081.
39. G. Yu, L. Hu, N. Liu, H. Wang, M. Vosgueritchian, Y. Yang, Y. Cui and Z. Bao, Nano Lett., 2011; 11: 4438–4442.
40. G. Yu, L. Hu, M. Vosgueritchian, H. Wang, X. Xie,J. McDonough, X.Cui, Y. Cui and Z. Bao, Nano Lett., 2011;11: 2905–2911.

41. J.-H. Kim, K. H. Lee, L. J. Overzet and G. S. Lee, Nano Lett.,2011; 11: 2611-2617. This journal is © The Royal Society of Chemistry 2014 J. Mater. Chem. A,2014,2,2985–2992 | 2991Paper Journal of Materials Chemistry A Published on 26 November 2013. Downloaded by McGill University on 21/10/2014 20:18:07. View Article Online
42. L. Bao, J. Zang and X. Li, Nano Lett., 2011;11:1215–1220.
43. Y. Hou, Y. Cheng, T. Hobson and J. Liu, Nano Lett., 2010; 10:2727-2733.
44. 44. De Gregorio G.F., Prado R., Vriamont C., Erdocia X., Labidi J., Hallett J.P., Welton T. Oxidative DE polymerization of lignin using a novel polyoxometalate-protic ionic liquid system. ACS Sustain. Chem.Eng. 2016;4:6031–6036. doi: 10.1021/acssuschemeng.6b01339. [CrossRef]
45. Fischer A.E., Pettigrew K.A., Rolison D.R., Stroud R.M., Long J.W. Incorporation of homogeneous, Nano scale MnO_2 within ultra porous carbon structures via self-limiting electro less deposition: Implications for electrochemical capacitors. Nano Lett. 2007;7:281–286. doi: 10.1021/nl062263i. [PubMed] [Cross Ref]
46. Leizhang, Hongdong Liu, Haibo Ruan, Yongyao S, Rong Hu, Liang Liang Tian, Zhongli H, JingLI Int. J.Electrochem.Sci, 2016; 11:10815-10826. Doi:10.20964/2016.12.82.
47. S. K. Park, H. J. Lee, M.H. Lee and H. S. Park, chem. Eng. J., 2015; 281:724.
48. S.K.Park, H.J.Lee, M.H. Lee and H.S.Park, chem.Eng.J., 2015; 281: 724.
49. H.Tao, L.Fan, Y.Mei and X.Qu, Electrochem, commun , 2011; 13:1332.
50. yongXu, Schoonen Martin AA. The absolute energy position ok conduction of valence band of selected semiconducting minerals. Am mineral 2000;85(3-4):543-56.
51. Wang Ming Yan, Huang Junrao, Tong Zhi Wei, Li Weihua, Chen Jun. journals of alloys and compounds. 2013; 568: 26-35.
52. M.panich, A.L. shames, T. nakaijima, on paramagnetic in fluorinated graphite. EPR and solid state NMR study, journal of physics and chemistry of solids 2001; 62
53. S. Eigler, dotzer, c.& Hirsch, A. Visalization of defect densities in reduced grapheme oxide carbon N.y., 2012; 50: 3666-3673.
54. S.j.Wang, Y.G., Q. zheng, J. K. Kim “fabrication of highly conducting and transparent grapheme films” carbon, 2010; 48:1815.
55. A. Gupta, G. Chen, P. Joshi, S. Tadigadapa, P. C. Eklund “Raman scattering from high-frequency phonons in supported n-grapheme layer films” Nan.LEH, 2006;6
56. LuizGustov DE OLIVERA LOPEZ CANLADO. Raman spectroscopy of Nano graphite, Sep 2006.

57. Z.HAo, C. Gaoping, W. Weikun, Y. Keguo, X. Bin, Z. Wenfeng, Y. Y sheng, Electrochemical.journal of Materials Science and Engineering, 2009; 54:1153